ICAS 2020 SHANG HAI
International Council of the Aeronautical Sciences
32nd Congress of the International Council of the Aeronautical Sciences
September 6-10, 2021
Pudong Shangri-La, Shanghai, China

Supersonic Aeroelastic Analysis of an All-movable Wing with Free Play

Kaihua Yuan[1], **Meng Cheng**[1]

[1]Beijing Electro-Mechanical Engineering Institute, Beijing100074, PR China.

Abstract

Nonlinear aeroelastic characteristics of an all movable wing with free play are investigated in this study. The wing model has a free play structural nonlinearity at its pitch axis. Nonlinear aerodynamic flows with unsteady shock waves are also considered in supersonic flow regions. The computational fluid dynamics/computational structural dynamics (CFD/CSD) coupling method is developed. To effectively consider the effects of free play structural nonlinearity, the fictitious mass method (FMM) is applied to structural vibration analysis based on finite element method(FEM). To solve the nonlinear aeroelastic governing equations, the time integration based on the algorithm of predictor-multi-corrector which can decrease the numerical error compared with the traditional loosed coupling method is used. Typical nonlinear responses of limit cycle oscillations(LCO) and phase plots are presented to show the complex effect of simultaneous fluid-structure nonlinearities. Results show that limit cycle oscillations are observed at velocity lower or greater than linear flutter speed. This importantly indicates the strong possibility of detrimental structural failures before reaching a conventionally predicted flutter dynamic pressure.

Keywords: free play nonlinearity, fictitious mass method, switching point, bisection method, limit cycle oscillation, CFD/CSD coupling

1. General Introduction

The field of aeroelasticity is an integration of a number of engineering disciplines which cover the interaction between elastic, inertial and aerodynamic loads on flexible aerospace structures. Flutter is a dynamic aeroelastic instability problem. If flutter occurs in flight, the aircraft structure may fail. Therefore it is important to predict the flutter characteristics accurately. During the past decades, most flutter analysis of three-dimensional wings have been performed under the assumption of structural linearity. However, due to the worn and loose phenomena of control surface connections, manufacturing tolerance, the free play is widely occurred. The free play nonlinearity which is a typical category of concentrated nonlinearities tends to give the most critical aeroelastic instabilities. Typically, nonlinear aeroelastic responses include limit cycle oscillations(LCO) and chaotic motion, etc.

Nonlinear aeroelastic analyses of a wing with concentrated nonlinearities have been performed by several investigators. Laurenson and Trn [1] used the describing function method to investigate the aeroelastic responses of a missile control surface with free play and showed that LCOs could occur below the linear flutter boundary. Kim and Lee [2,3] investigated LCO and chaotic motion of a missile control surface and a 2-D flexible airfoil with free-play nonlinearity using time-domain analysis. Sheta et al. [4] studied a nonlinear aeroelastic system with a fifth-order polynomial spring using both computational and experimental methods. Bae et al. [5] investigated the nonlinear aeroelastic characteristics of a wing with free play using frequency and time domain analyses. It was shown that LCO and chaotic motion are observed in a wide range of air speeds below the linear boundary. Dowell et al.[6] studied the transonic LCO behavior of a three DOFs aeroelastic wing model with free play in its control surface deflection. Munteanu et al.[7] using the reduced order model (ROM)method to research the LCOs for an aeroelastic airfoil with structural nonlinearity in subsonic and transonic air flow. Chen et al.[8] studied a delta wing model with geometrical nonlinearity in transonic air flow, and a new nonlinear aeroelastic model was developed in their work.

There are semi-analytical and numerical methods which are used for the flutter analysis of nonlinear aeroelastic systems with free-play nonlinearity. Describing function [9], time–frequency [10],

harmonic balance [11], perturbation [12], center manifold and time marching integration methods.

The purpose of the present study is to investigate the aeroelastic problems of an all-movable wing including both the structural nonlinearity and the aerodynamic nonlinearity. The finite element method is used for the structural analysis and the modal approach using fictitious mass method [13] is used to increase computational efficiency. The computational fluid dynamics (CFD) technique is used for the computation of unsteady aerodynamic forces. To solve the nonlinear aeroelastic governing equations, the time integration based on the algorithm of predictor-multi-corrector is used. The nonlinear aeroelastic characteristics of an all-movable wing are studied.

2. Theoretical Background

2.1 Aeroelastic Modeling

The aeroelastic equations of motion for an elastic wing can be written as:

$$\boldsymbol{M}\ddot{\boldsymbol{u}} + \boldsymbol{C}\dot{\boldsymbol{u}} + \boldsymbol{K}(u)\boldsymbol{u} = \boldsymbol{F} \tag{1}$$

where $\boldsymbol{M}$, $\boldsymbol{C}$, $\boldsymbol{K}$, $\boldsymbol{u}$, $\boldsymbol{F}$ are the mass matrix, damping matrix, stiffness matrix, displacement vector, and aerodynamic force vector, respectively. For piecewise nonlinearity (Figure 1), nonlinear stiffness matrix can be written as follows:

$$\boldsymbol{K}(u) = \boldsymbol{K}_l(u) + \boldsymbol{f}(\delta) \tag{2}$$

where $\boldsymbol{K}_l(u)$ is a linear stiffness matrix of the all movable wing without free play stiffness, and $f(\delta)$ is the nonlinear restoring force vector whose element are zero except for the nonlinear contribution. For a free play nonlinearity, $f(\delta)$ is given as follows:

$$\boldsymbol{f}(\delta) = \begin{cases} k_\delta(\delta - d) & \delta > d \\ 0 & -d \le \delta \le d \\ k_\delta(\delta + d) & \delta < -d \end{cases} \tag{3}$$

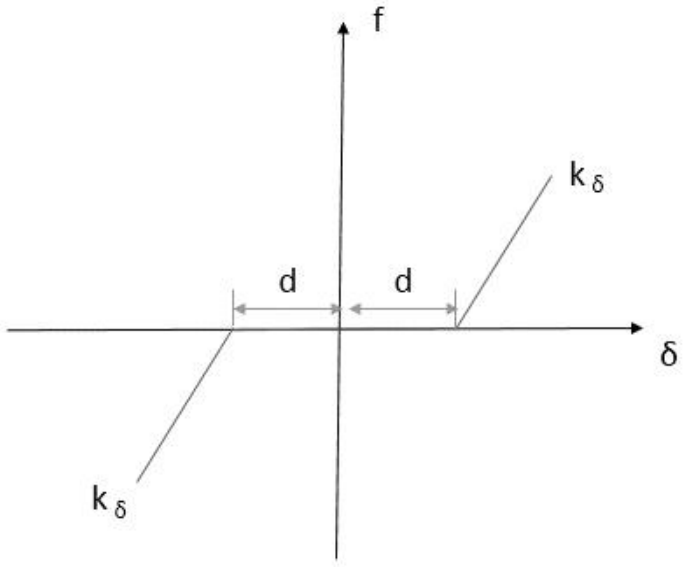

Figure 1 – Relationship between restoring moment and rotation angle for free play nonlinearity

2.2 Normal Modes of the Fictitious Mass Method

In nonlinear aeroelastic problems with concentrated structural nonlinearities, structural stiffness are varying as the displacement changes. Therefore, using a constant normal mode from a fixed structural model gives inaccurate results. To overcome this problem, the fictitious mass method (FMM) is used in this study. The idea of the FMM is that the local deformation due to the large mass enables us to examine the structural variation. Ignoring the damping and aerodynamic force terms in Eq., the free equation of motion of an *n* degrees of freedom nominal undamped structure loaded with fictitious mass is

$$\left(\boldsymbol{M}+\boldsymbol{M}_f\right)\ddot{\boldsymbol{u}}+\boldsymbol{K}\boldsymbol{u}=\boldsymbol{0} \tag{4}$$

where the elements of the fictitious mass matrix $\boldsymbol{M}_f$ are zero except for the terms added to the structure at the locations of subsequent large structural variations. From the normal mode analysis using a finite element method, the displacement vector $\boldsymbol{u}$ is a linear combination of the fictitious mass modes, namely $\boldsymbol{u}=\boldsymbol{\phi}_f q_f$ .The generalized mass and stiffness matrix are given as

$$\overline{\boldsymbol{M}}_f=\boldsymbol{\phi}_f^{\,T}\left(\boldsymbol{M}+\boldsymbol{M}_f\right)\boldsymbol{\phi}_f \tag{5}$$

$$\overline{\boldsymbol{K}}_f=\boldsymbol{\phi}_f^{\,T}\boldsymbol{K}\boldsymbol{\phi}_f=\omega_f^2\overline{\boldsymbol{M}}_f \tag{6}$$

where $\boldsymbol{\omega}_f$ is a diagonal matrix of the natural frequencies including zero frequencies for rigid-body modes.

Using above transformation equation, the actual structure with concentrated local stiffness variations (without fictitious massed) can be written as

$$\boldsymbol{\phi}_f^{\,T}\left(\boldsymbol{M}-\boldsymbol{M}_f\right)\boldsymbol{\phi}_f\ddot{q}_f+\boldsymbol{\phi}_f^{\,T}\left(\boldsymbol{K}+\Delta\boldsymbol{K}\right)\boldsymbol{\phi}_f q_f=\boldsymbol{0} \tag{7}$$

Substitution of Eq.(5) and Eq.(6) in Eq.(7)

$$\left(\overline{\boldsymbol{M}}_f-\boldsymbol{\phi}_f^{\,T}\boldsymbol{M}_f\boldsymbol{\phi}_f\right)\ddot{q}_f+\left(\overline{\boldsymbol{K}}_f+\boldsymbol{\phi}_f^{\,T}\Delta\boldsymbol{K}\boldsymbol{\phi}_f\right)q_f=\boldsymbol{0} \tag{8}$$

From above equations, we obtain natural frequencies $\boldsymbol{\omega}_b$ of the actual structure and the associated square eigenvector matrix $\boldsymbol{\chi}_b$. Since an all movable wing model is considered in this study, a finite element modal is taking account of the stiffness variation at the pitch axis.

The fictitious mass modes can serve as a constant set of generalized coordinates for a wide range of additive and subtractive structural variations in the vicintiy of the fictitious masses. For computational convenience, let us define the following base modal matrix as

$$\boldsymbol{\phi}_b=\boldsymbol{\phi}_f\boldsymbol{\chi}_b \tag{9}$$

The eigenvectors are normalized to yield a unit generalized mass matrix.

$$\overline{\boldsymbol{M}}_b=\boldsymbol{\chi}_b^{\,T}\left(\overline{\boldsymbol{M}}_f-\boldsymbol{\phi}_f^{\,T}\boldsymbol{M}_f\boldsymbol{\phi}\right)\boldsymbol{\chi}_b=\boldsymbol{I} \tag{10}$$

Using Eq.(8), Eq.(9) and Eq.(10), the aeroelastic equations of motion for an elastic wing with concentrated structural nonlinearity is written as:

$$\overline{\boldsymbol{M}}_b\ddot{q}+\overline{\boldsymbol{C}}_b\dot{q}+\overline{\boldsymbol{K}}_b q=\overline{\boldsymbol{F}}\left(t,q,\dot{q}\right) \tag{11}$$

Where $\overline{\boldsymbol{M}}_b=\boldsymbol{\chi}_b^{\,T}\left(\overline{\boldsymbol{M}}_f-\boldsymbol{\phi}_f^{\,T}\boldsymbol{M}_f\boldsymbol{\phi}\right)\boldsymbol{\chi}_b$, $\overline{\boldsymbol{C}}_b=2\xi_b\omega_b$, $\overline{\boldsymbol{K}}_b=\boldsymbol{\chi}_b^{\,T}\overline{\boldsymbol{K}}_f\boldsymbol{\chi}_b+\boldsymbol{\phi}_b^{\,T}\boldsymbol{f}\left(\delta\right)$, $\overline{\boldsymbol{F}}=\boldsymbol{\phi}_b^{\,T}\boldsymbol{F}$.

$\boldsymbol{F}$ is the external force vector due to unsteady aerodynamic flows around the wing. It is computed on the CFD grids of the wing surface. Using transformation matrix $\boldsymbol{Q}_{as}$ for surface spline of modal matrix from FEM node to CFD grid, then $\overline{\boldsymbol{F}}=\tilde{\boldsymbol{\phi}}_b^{\,T}\boldsymbol{Q}^T_{as}\tilde{\boldsymbol{F}}$. $\tilde{\boldsymbol{F}}$ can be obtained by solving Navier-

Stokes equation.

2.3 State-space Form of Aeroelastic Equation and Time Simulation

To integrate the aeroelastic equations in Eq., a transformation is applied to obtain state-space equations. Introducing the state vector $\boldsymbol{E}$ to perform the efficient numerical calculation, Eq.(11) can be written in the first order form as

$$\dot{\boldsymbol{E}} = \eta(\boldsymbol{E},t) = \boldsymbol{A}\cdot\boldsymbol{E}(\boldsymbol{E},t) + \boldsymbol{B}\cdot\boldsymbol{P}(\boldsymbol{E},t) \tag{12}$$

Where $\boldsymbol{A} = \begin{bmatrix} \boldsymbol{0} & \boldsymbol{I} \\ -\bar{\boldsymbol{M}}_b^{-1}\boldsymbol{\chi}_b^{T}\bar{\boldsymbol{K}}_f\boldsymbol{\chi}_b & -\bar{\boldsymbol{M}}_b^{-1}\bar{\boldsymbol{C}}_b \end{bmatrix}$, $\boldsymbol{B} = \begin{bmatrix} \boldsymbol{0} \\ \bar{\boldsymbol{M}}_b^{-1} \end{bmatrix}$, $\boldsymbol{P} = \begin{bmatrix} \boldsymbol{0} \\ \bar{\boldsymbol{F}} - \boldsymbol{\phi}_b^{T}\boldsymbol{f}(\delta) \end{bmatrix}$, $\boldsymbol{E} = \begin{bmatrix} q \\ \dot{q} \end{bmatrix}$.

For the nonlinear aeroelastic systems, the time integration is based on the algorithm of predictor-multi-corrector be used to calculate the time response of Eq. .

$$\begin{cases} \bar{\boldsymbol{E}}_{n+1} = \boldsymbol{E}_n + \dfrac{\Delta t}{24}\left(55\eta_n - 59\eta_{n-1} + 37\eta_{n-2} - 9\eta_{n-3}\right) \\ \boldsymbol{E}_{n+1} = \boldsymbol{E}_n + \dfrac{\Delta t}{24}\left[9\eta_{n+1}\left(\bar{\boldsymbol{E}}_{n+1,}t+\Delta t\right) + 19\eta_n - 5\eta_{n-1} + \eta_{n-2}\right] \end{cases} \tag{13}$$

3. Numerical Results and Discussion

Figure 2 shows an all movable wing with free play. The chord length of the wing root is 0.5*m*, the chord length of the wingtip is 0.15*m* , the length of the wing span is 0.28 *m,* and swept-back angle of leading edge is 45° . The material of wing is aluminum alloy and its properties are E=72.4 GPa, v=0.33, and ρ=2700kg/m^3. The finite element structural model is built up from solid, plate, beam, spring, and concentrated mass elements. The wing is connected by a spindle axis with an equivalent torsional spring. The first mode is the bending mode. The frequency is 73.8Hz. The second mode is the torsional mode. The frequency is 86.1Hz.

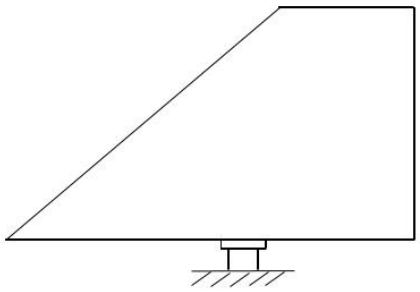

Figure 2 – Geometric configuration of the wing

3.1 Linear Aeroelastic Analysis

Figure 3 compares aeroelastic responses of a linear structure model with same Mach numbers (Ma=2.0) at two-different initial condition (Case1: $\dot{q}_1 = 0.05$, $\dot{q}_2 = -0.05$. Case2: the initial torsion angle is 0.6°). Flutter dynamic pressure and frequency are same at different initial condition (Flutter dynamic pressure is 142Kpa, flutter frequency is 79.6Hz), where the amplitude of the tip trailing edge are not equal.

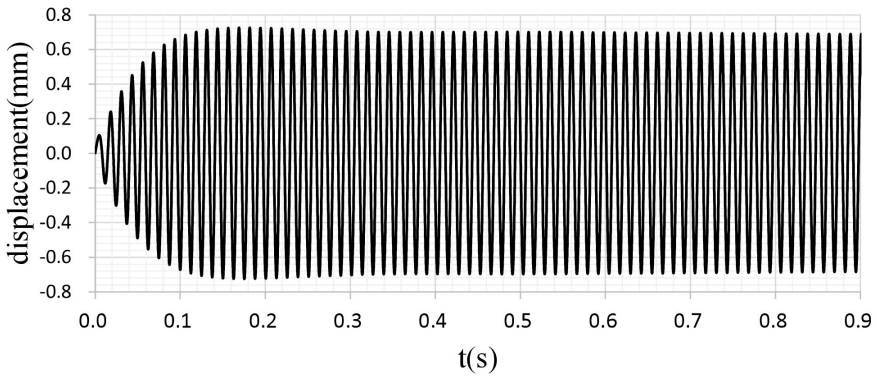

(a) Case 1

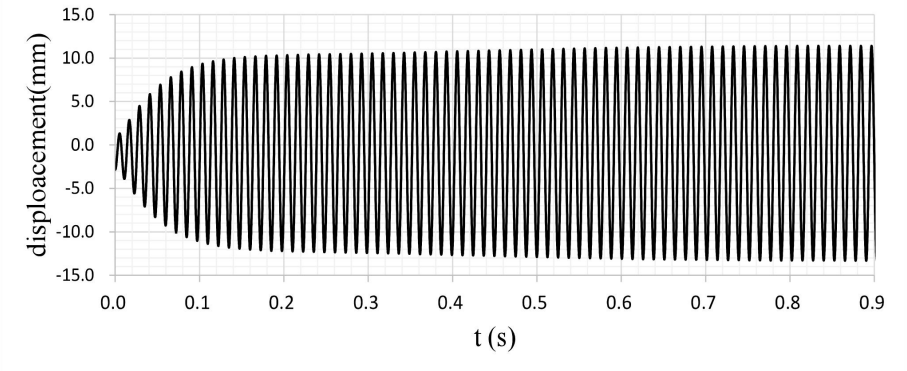

(b) Case 2

Figure 3 – Aeroelastic responses of a linear structure model

3.2 Nonlinear Aeroelastic Analysis of different dynamic pressure

To investigate the nonlinear aeroelastic characteristics of the all movable wing, the aeroelasticity are calculated with the same Mach (Ma=2.0), the same free play angle ($\delta = 0.2^{\circ}$) and the same initial conditions (the initial torsion angle is 0.4°) at different dynamic pressure.

Figure 4 shows aeroelastic responses of the tip leading edge. The nonlinear aeroelastic analysis under different dynamic pressure conditions shows that: The wing has entered the LCO state when the dynamic pressure is lower than the linear flutter boundary. With the increase of dynamic pressure, the amplitudes of structural and aerodynamic responses of the wing increase, and the flutter frequency of the LCO increases continuously.

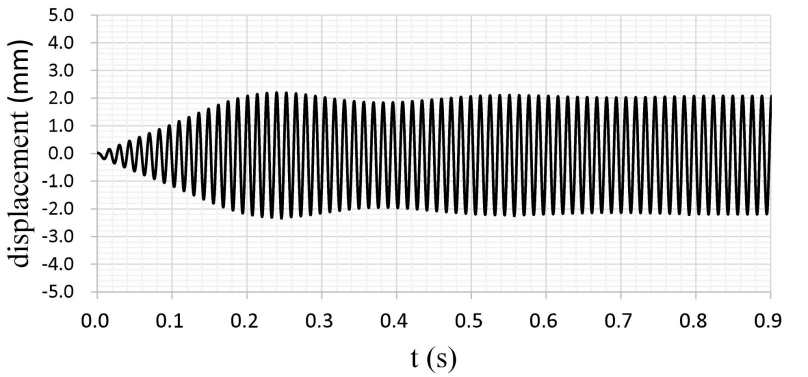

(a) Case 1: dynamic pressure 75Kpa, response frequency 77.12Hz

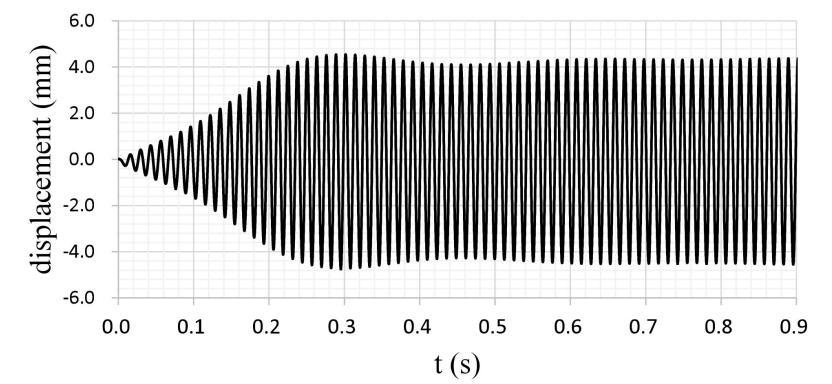

(b) Case 2: dynamic pressure 110Kpa, response frequency 78.33Hz

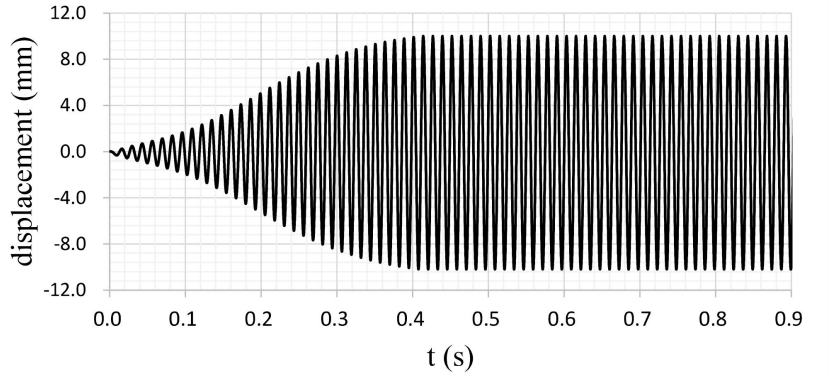

(c) Case 3: dynamic pressure 125Kpa, response frequency 79.11Hz

Figure 4 – Nonlinear aeroelastic responses of different dynamic pressure

3.3 Nonlinear Aeroelastic Analysis of different free play angles

Nonlinear aeroelastic computations in Ma 2.0 have been conducted for different free play angles: $\delta = 0.1^{\circ}, \delta = 0.2^{\circ}$ and $\delta = 0.4^{\circ}$ .Figure 5 shows computed nonlinear responses with the same initial conditions (the initial torsion angle is 0.6°) and the same dynamic pressure at the different free play angles. The comparison of aeroelastic responses of different free play angles is shown in the figure below, which shows that: When the initial displacement is large enough, the LCO can be fully excited. The larger the free play angle is, the larger the initial excitation is needed to excite the aeroelastic response. When the LCO is excited, the larger the free play angle is, the larger the response amplitude is. Whereas the response frequency of different free play angles is the same. When the LCO cannot be fully excited, the response frequency is relatively low.

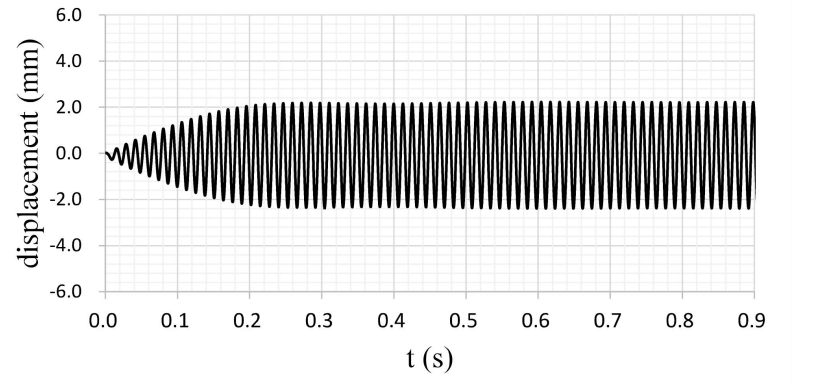

(a) Case 1: $\delta = 0.1^{\circ}$, response frequency 78.33Hz

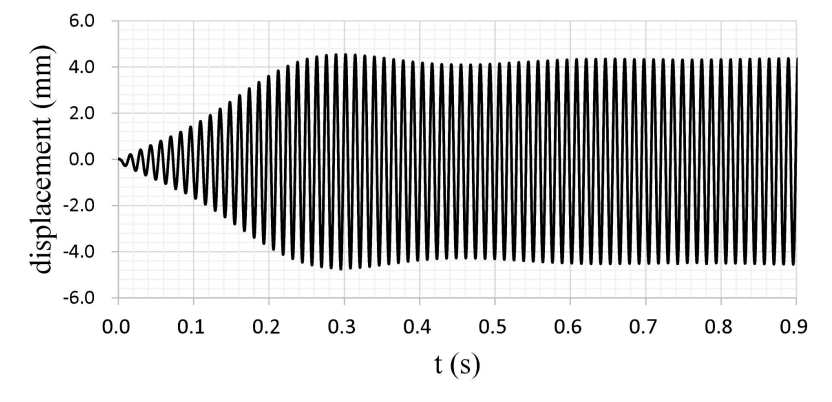

(b) Case 2: $\delta = 0.2^{\circ}$, response frequency 78.33Hz

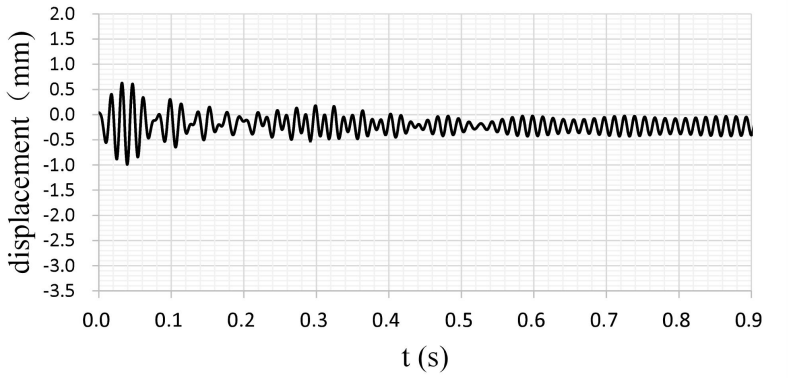

. Figure 5 – Nonlinear aeroelastic responses of different free play angles

4. Conclusions

In the present study, the nonlinear aeroelastic analysis of an all movable wing is performed. The finite element method is used for the analysis of the structure. A modal approach using the fictitious mass method is used to save computation time and memory. The computational fluid dynamics/computational structural dynamics (CFD/CSD) coupling method is developed. To solve the nonlinear aeroelastic governing equations, the time integration is based on the algorithm of predictor-multi-corrector is used. For the all movable wing, the wing has entered the LCO state before the linear flutter dynamic boundary. The results physically show that the dynamic pressure and the free play angles have a significant effect on the aeroelastic responses. Therefore, as for a safe and good performance design of an all-movable wing, it is necessary to conduct accurate analyses and investigate the complex characteristics of fluid-structure nonlinearities in detail.

References

[1] Laurenson R M, Trn R M. Flutter Analysis of Missile Control Surfaces Containing Structural Nonlinearities. AIAA Journal, Vol. 18, No. 10, pp. 1245–1251,1980.

[2] Lee I, Kim S H. Aeroelastic analysis of a flexile control surface with structural nonlinearity. Journal of Aircraft, Vol. 32, pp. 868–874, 1995.

[3] Kim S H, Lee I. Aeroelastic Analysis of a Flexible Airfoil with a Free play Nonlinearity. Journal of Sound and Vibration, Vol. 193, No. 4,, pp. 823–846, 1996.

[4] Sheta EF, Harrand VJ, Thomson D E, Strganac TW. Computational and experimental investigation of limit cycle oscillations of nonlinear aeroelastic systems. Journal of Aircraft, Vol. 39, pp.133–141, 2002.

[5] Bae J S, Yang S M, Lee I. Linear and Nonlinear Aeroelastic Analysis of Fighter-Type Wing with Control Surface. Journal of Aircraft, Vol. 39, No. 4, pp. 697–708, 2002.

[6] Dowell E H, Thomas J P. Hall KC. Transonic limit cycle oscillation analysis using reduced order aerodynamic models. Fluids Struct, Vol. 19, pp.17–27,2004.

[7] Munteanu S, Rajadas J, Nam C, Chattopadhyay A. Reduced-order-model approach for aeroelastic analysis involving aerodynamic and structural nonlinearities. AIAA Journal, Vol. 43, pp. 560–571, 2005.

[8] Chen T, Xu M, Xie L. Aeroelastic modeling using geometrically nonlinear solid-shell elements. AIAA Journal, Vol. 52, pp.1980–1993, 2014.

[9] He S, Yang Z, Gu Y. Limit cycle oscillation behavior of transonic control surface buzz considering free-play nonlinearity. Journa of Fluids and Structures. Vol. 61, pp. 431–449, 2016.

[10] Dimitriadis G, Cooper J E. A time–frequency technique for the stability analysis of impulse responses from nonlinear aeroelastic systems. Journal of Fluids and Structures. Vol. 17, pp. 1181–1201, 2003.

[11] Liu L, Dowell E H. Harmonic balance approach for an airfoil with a free play control surface. AIAA Journal, Vol. 43, pp. 802–815, 2005.

[12] Dessi D, Mastroddi F. Limit-cycle stability reversal via singular perturbation and wing-flap flutter. Journal of Fluids and Structures. Vol. 19, pp.765–783, 2004.

[13] Karpel M, Wieseman C D. Modal Coordinates for Aeorelastic Analysis with Large Local Structural Variations. Journal of Aircraft, Vol. 31, No. 2, pp. 396-400, 1994.

Copyright Statement